Title
Calibration and assessment of process-based numerical models for beach profile evolution in southern California

Permalink
https://escholarship.org/uc/item/0tr2v6np

Authors
Kalligeris, N
Smit, P
Ludka, B C
et al.

Publication Date
2018

Data Availability
The data associated with this publication are available upon request.

Peer reviewed

Calibration and assessment of process-based numerical models for beach profile evolution in southern California

N. Kalligeris[a,*], P. Smit[b], B. C. Ludka[c], R. T. Guza[c], T. W. Gallien[a,c]

[a]*Department of Civil and Environmental Engineering, University of California, Los Angeles, CA, USA*
[b]*Spoondrift Technologies, Inc., Half Moon Bay, CA, USA*
[c]*Scripps Institution of Oceanography, University of California, San Diego, La Jolla, CA, USA*

Abstract

Cross-shore profile response to energetic wave events is challenging to predict because the physics are poorly understood and wave and topographic data are often sparse or unknown. Six events with varying duration, wave intensity and beach slopes are used to calibrate and assess two process-based cross-shore models, CShore and XBeach, at two southern California beaches. Model performance is quantitatively evaluated using high resolution temporal-spatial survey observations along with Brier Skill Scores (BSS) and a novel Bulk Shoreline Change Error (BSCE) metric that considers alongshore-averaged upper beach volume. XBeach is tested with default and site-calibrated parameters. Site calibration improved XBeach model skill, however the XBeach skill scores are still often low and in no case was the offshore bar correctly predicted. Notably XBeach calibration is sensitive to depth extent and produces significantly different model skill for upper beach and full profile predictions. For CShore, the better performing of two existing sets of parameter values is used. CShore and XBeach predict profile change with limited skill. In their present forms, CShore and XBeach are unable to accurately predict beach profile change on these typical southern California beaches, but when calibrated may provide qualitatively useful estimates of bulk shoreline erosion.

---

[*]Corresponding author
Email address: `nkalligeris@ucla.edu` (N. Kalligeris)

1. Introduction

Sandy beaches protect backbeach structures from flooding and erosion and contribute to recreational tourist economies worldwide. The estimated recreational value of California beaches is ∼\$5 billion annually [1]. Concomitant pressures of urbanization, rising seas [2, 3, 4, 5, 6] and potentially changing wave climates [e.g. more frequent El Niño winters bringing energetic wave conditions to coastal California; 7, 8, 9, 10] will dramatically increase coastal vulnerability mitigation planning efforts that incorporate beach evolution modeling [11], particularly during energetic storm events.

Modeling beach profile evolution is challenging; waves are irregular and nonlinear, fluid flows are turbulent, sediment grains vary in shapes and size and initial beach states are often not fully resolved. Beach evolution models range from empirical relations between offshore wave conditions and the evolution of the profile shape [12, 13, 14, 15] to wave phase resolving models that incorporate inter-granular interactions and turbulent suspension [16, 17, 18, 19]. As spatial and temporal scales increase, physical processes are increasingly parameterized due to computational and theoretical limitations. The present state-of-the art 'process-based models' project energetic event impacts over a time span of days; sand level changes are estimated from wave-driven cross-shore gradients of parameterized net sediment fluxes. Although these models attempt to explicitly describe the relevant dynamics, in practice they are semi-empirical both for efficiency reasons, and because the important physics are incompletely understood. Observations are essential to assess model performance under a range of conditions.

Here two morphodynamic models, CShore [20] and XBeach [21] are applied to predict cross-shore profile evolution at two southern California beaches over several days. Both CShore and XBeach estimate the morphological impact of

events with time-scales of storms on sandy beaches [22, 23]. However, the parameterization level differs significantly. CShore assumes quasi-stationary hydrodynamics and that sea-swell frequencies dominate runup motions. In particular, runup estimates are applicable to steep slopes [20], arguably limiting CShore to reflective and intermediate conditions. In contrast, XBeach was designed to efficiently simulate the hydrodynamics under the assumption of a saturated surf zone [24], and explicitly accounts for infra-gravity (IG) timescale physics. As a consequence, XBeach is limited in application to dissipative, IG-dominated beaches [e.g. 21, 25]. In spite of these restrictions, both models have been applied outside of their application range before with moderate success: XBeach to intermediate beaches [26, 27], and CShore to dissipative conditions [28].

Typical foreshore slopes for San Diego County beaches along the Torrey Pines-Cardiff coastline range from 1/20 to 1/50 [29]. The wave climate is dominated by energetic swell events and beaches range from dissipative to intermediate states [12, 30]. Both CShore and XBeach have been applied with success in southern California. CShore predicted storm impact of the January 1988 storm at Oceanside and Del Mar beaches [22] – with pre-storm foreshore profiles of $\sim 1/35$. XBeach was applied successfully to a November 2001 storm-event at Torrey-Pines beach which served as a validation case for the integration of XBeach in the COSMOS framework assessing climate change-related coastal impacts on the California coast [31, 32]. However, Torrey-Pines beach was nourished prior to the November 2001 storm, and consequently was in an unnatural state (section 2.4).

This work examines the performance of XBeach and CShore for typical moderate storm events in southern California on beaches with foreslopes of 1/20-1/30. CShore and XBeach are tested for six selected storm events using high quality, comprehensive survey data from the backbeach to 8 m depth, collected shortly before and after storm waves. The data set facilitates model evaluation for both subaerial and full beach profiles. In some cases, daily subaerial profiles were measured, allowing consideration of numerical error accumulation. To obtain representative model skill we select the best performing CShore parameter

set from two possible configurations given by model authors [found after exten-
sive calibration across sites; 22]. XBeach parameter selection guidance is less
clear [literature XBeach applications typically involve site-specific calibration,
e.g. 33, 34, 25, 35], therefore we conduct extensive calibration for XBeach to
find optimal parameters. In what follows we will introduce events and sites
considered, models and model setup, and skill criteria in section 2. Next, we
present model results (section 3), discuss implications (section 4) and summarize
findings (section 5).

2. Methods

2.1. Study beaches

Cardiff and Torrey Pines State Beaches (Fig. 1) range from dissipative
to intermediate states [classification of 12, 30], with shallow offshore slopes
($\sim 1/100$) [36], and foreshore slopes in the swash region between $1/20$ and $1/50$
[29]. Foreshore slopes vary as the swash zone migrates with water levels along
the typically concave beach face, which also has slopes that vary seasonally and
alongshore. The sand is medium grained (median $D_{50} = 0.20 \pm 0.05$ mm), with
cobbles intermittently exposed, predominately when the subaerial beach is in an
eroded state. Patches of offshore rocky reef were identified using sidescan sonar
[37] and as less erodible surfaces in bathymetry surveys [38]. Section T7 has
submerged rocky reef and is cliff-backed, whereas sections T8 and C2 are sandy,
backed by road and riprap, and typically exhibit 1-D cross-shore behavior [15].

2.2. Sand levels

Monthly subaerial (between backbeach and the low tide waterline) sand ele-
vations along shore-parallel tracks with 10 m spacing, and quarterly bathymetry
(between backbeach and $\sim$8 m depth) surveys with 100 m spaced shore-
perpendicular transects were measured using GPS-equipped vehicles. Addi-
tional partial bathymetry surveys (between backbeach and $\sim$3 m depth) were
conducted along the 100 m spaced shore-perpendicular transects. Occasionally

4

surveys were performed a few days apart. The data were mapped to a uniform grid with 100 m alongshore spacing, and gaps filled (Fig. 1c-d), following Ludka et al. [38]. Sand levels vary seasonally (blue curves, Fig. 2b, 3b).

2.3. Waves

Southern California waves vary seasonally (Fig. 2a, 3a), with larger N. Pacific winter swell (associated with the Aleutian low) and less energetic summer swell from the S. Pacific. Fair-weather winds generate waves of intermediate height and period. Local summer sea breeze generates smaller, shorter period waves [39]. Incident wave condition estimates in 10 m water depth are used to drive morphological change models. Wave spectra and low order directional moments were extracted from the Coastal Data Information Program (CDIP) wave prediction system [40, 41]. Deep water buoys, offshore of the Channel Islands (Fig. 1a), are used to initialize a linear swell ($f = 0.0378 - 0.0875$ Hz) model that accounts for bathymetric refraction and island blocking, and neglects generation and dissipation. Local buoys (e.g. buoy 46225 in Fig. 1b) are used to drive a sea model ($f = 0.0875 - 0.5$ Hz). The swell model is necessary, in addition to the local buoys, because complex bathymetric refraction and island shadowing causes sharp spatial wave height gradients. Hourly directional spectra were derived from Monitoring and Prediction locations (MOPs) in 10 m depth, spaced 100 m alongshore, using the Maximum Entropy Method [MEM, 42], that creates narrow directional peaks appropriate in swell-dominated wave climates [41].

2.4. Event description

Cardiff and Torrey Pines beaches exhibit equilibrium behavior, with profile response governed both by incident wave conditions and the beach state [43, 44, 15]. Eroded and accreted beaches respond differently to the same waves. A simple empirical beach state model (black curve) previously calibrated on these beaches [15] predicts subaerial erosion (Fig. 2b, 3b) when $H_s > H_{eq}$ (Fig. 2a,
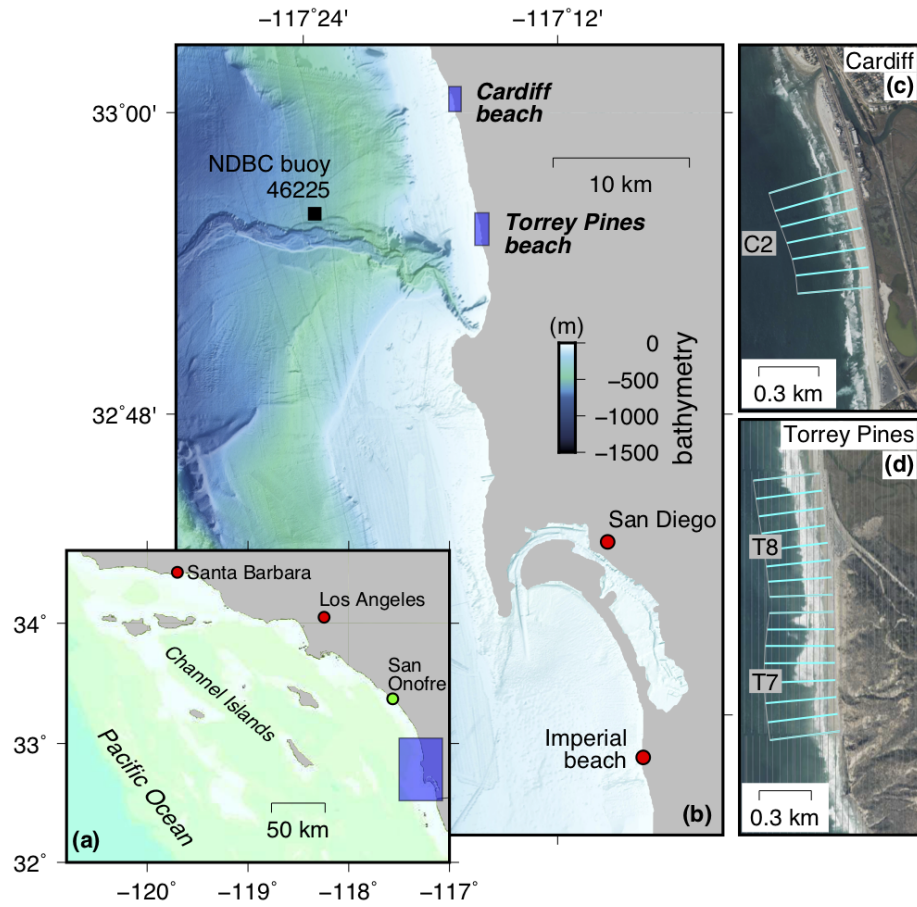
Figure 1: (a-b) Location of Torrey Pines and Cardiff beaches, in southern California. (c-d) Location of the cross-shore survey transects (cyan lines) overlaid on orthophotos. Survey section names are indicated.

3a). The equilibrium model does not account for nourishment, and Section T8 (dark blue,2b) was nourished in 2001 [45, 43].

Six events with high temporal resolution surveys were selected (Fig. 2d-i, 3d-f, Table 1): one 4-day event at Torrey-Pines (event I), four events of varying intensity and duration at Cardiff Beach (events II-V), and another 2-day event at Torrey-Pines for which the upper beach of section T8 had recently been nourished (event VI). Section T7 has submerged rocky reef and is only modeled for event VI. During all events, the subaerial beach was relatively accreted (steep) when compared with the typical seasonal variability. The observed erosion rate between surveys (Fig. 2f,i, 3f) was highest during events I, II and III, (partially due to survey timing), and weak during events IV and V. During all events, H_s exceeded the modeled H_{eq} at least some of the time (beach state A correspondingly decreases in Fig. 3e)

The November 2001 storm event (VI) represents an atypical beach behavior due to the nourishment project which had taken place in April 2001. The beach fill region and adjacent areas experienced substantial erosion during the 3-day storm event with significant wave height that peaked at 3.2 m [45]. Observed erosion was not alongshore-uniform, with erosion embayments, and steep sand peninsulas forming during high tide in the fill region [45]. This highly-2D morphological evolution of the beach face cannot be captured by 1-D models, however, promising profile evolution was presented by Barnard et al. [31] using XBeach1D.

Hourly wave conditions in 10 m depth, reverse-shoaled to deep water and coupled with hourly swash zone beach slopes between 1/20-1/29, result in average Iribarren numbers between $\xi_0 \sim 0.4 - 0.87$ (Table 1), where $\xi_0 = \frac{\beta}{\sqrt{H_0/L_0}}$ with H_0 and L_0 deep water wave height and wavelength, respectively. Based on Torrey Pines observations [Fig. 5 in 36], the event-averaged R^{IG}/R ratios are above 0.8 for all individual beach transects. The standard deviation of R^{IG}/R (Table 1), fluctuates during each event primarily due to the varying beach foreslope at different tidal levels. Along the dissipative Dutch coast the average ratio of infragravity to total swash is $R^{IG}/R \approx 0.85$ [46]. In this study, during high

7

tide the ratio is below 0.8 for all events except V and section T7 of event VI, indicating dissipative environmental conditions for event V and mildly-dissipative to dissipative environmental conditions for all other events, depending on the tidal level.

₁₅₀ *2.5. XBeach model*

XBeach [21] is a process based flow and sediment transport model used primarily to model erosion, overwash or barrier breaching during extreme storm events [e.g. 21, 47, 33]. Several open source XBeach versions have been released subsequently, and two hydrodynamic solvers were added [24]. Here, we employ ₁₅₅ the Kingsday XBeach release in 1-D surfbeat mode, which solves a time dependent wave action balance that forces a Generalized Lagrangian Mean (GLM) formulation of the nonlinear shallow water equations [48]. This formulation includes both sea-swell and infragravity waves. Roelvink et al. [23] describe in detail the hydrodynamic and sediment transport formulations employed here.

₁₆₀ The performance of XBeach (and CShore) with typical, southern California winter storm waves is examined. Site-specific calibration is used here to improve model skill, as in most applications of XBeach [24, and references therein]. The several dozen free parameters influencing beach evolution provide a wide parameter space to calibrate model predictions to a given set of field observations. ₁₆₅ Some model parameters were varied (Table 2, see Appendix A.1 for brief parameter descriptions), while other model parameters were set at default. The varied parameters were identified through a literature review and sensitivity analysis. All possible combinations of calibration parameter values result in 256 simulations for each test case. XBeach simulations, run in serial mode (with an ₁₇₀ AMD Opteron 6276 processor) on a high-performance computing cluster, took ~ 9 minutes to complete a day's real-time simulation for each test case on each beach transect.

XBeach was calibrated separately with two energetic (for the study area) events: Torrey Pines event I and Cardiff event V. Optimal parameters from the ₁₇₅ two full beach profile calibrations are quite similar, with the exception of one

8

Event	H_0 (m)	T_p (s)	H_0/L_0	β	ξ_0	R^{IG}/R
I	1.1-1.4	14.5-15.5	0.003-0.004	0.039-0.048	0.66-0.83	0.82(0.13)-0.90(0.11)
II	0.9-1.0	10.8-11.5	0.006-0.006	0.041-0.047	0.60-0.71	0.86(0.14)-0.90(0.11)
III	1.0-1.3	15.5-16.1	0.003-0.003	0.038-0.048	0.72-0.87	0.81(0.16)-0.87(0.12)
IV	0.8-0.9	11.7-12.6	0.004-0.005	0.035-0.048	0.59-0.83	0.81(0.17)-0.90(0.11)
V	1.1-1.1	9.1-9.3	0.008-0.009	0.035-0.041	0.40-0.48	0.96(0.05)-0.98(0.02)
VI	1.6-2.3	15.7-16.7	0.004-0.006	0.029-0.051	0.45-0.75	0.86(0.08)-0.98(0.01)

Table 1: Environmental conditions averaged over the duration of each event. Value range is over individual transects and R^{IG}/R values in parenthesis indicate standard deviation (over the event duration). Wave conditions in 10 m depth were reverse-shoaled to deep water, slope β is in swash zone, and Iribarren number $\xi_0 = \frac{\beta}{\sqrt{H_0/L_0}}$.
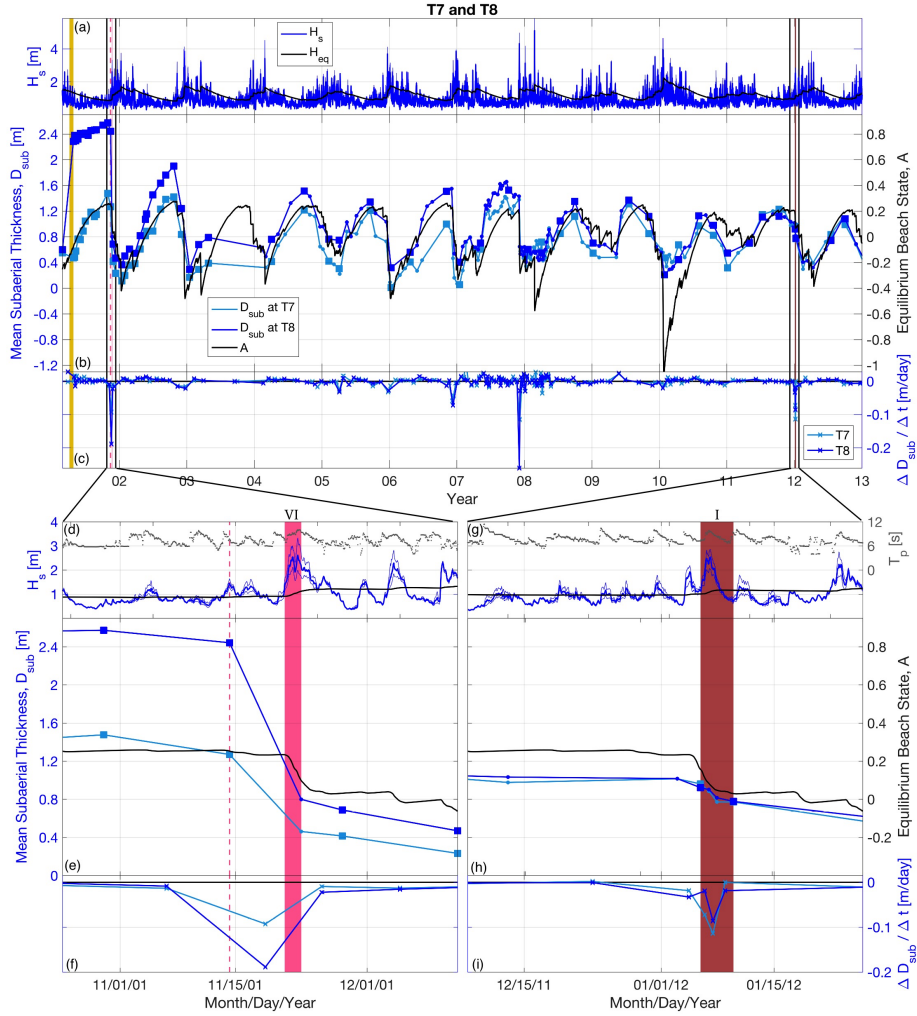
Figure 2: (a) Mean (thick blue), min and max (thin blue) significant wave height across sections T7 and T8 (15 cross-shore transects, Fig 1c,d). Equilibrium wave height, alongshore averaged over T7 and T8 (black). (b) Observed mean subaerial sand thickness (Surveyed surface from mean horizontal MSL position to backbeach, minus surface at MSL, divided by survey area) for T7 (light blue) and T8 (dark blue). Surveys are marked as full bathymetric (square), partial bathymetric (triangle),and subaerial (small circles). Dashed vertical lines show full profile surveys used to fill in missing initial offshore data when necessary. Modeled beach state (black) is forced with mean H_s (thick blue, panel a). (c) Observed change rate of mean subaerial thickness. (d-i) Zoom on events. Colored vertical strips span the test periods.
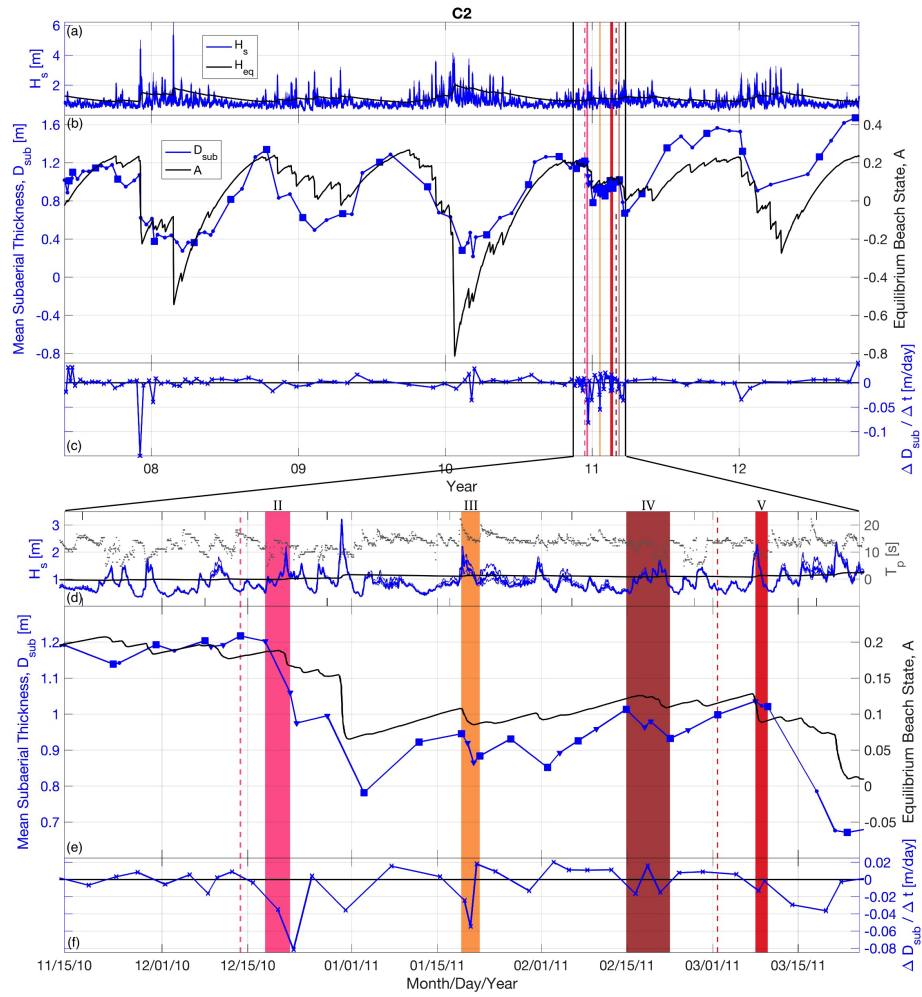
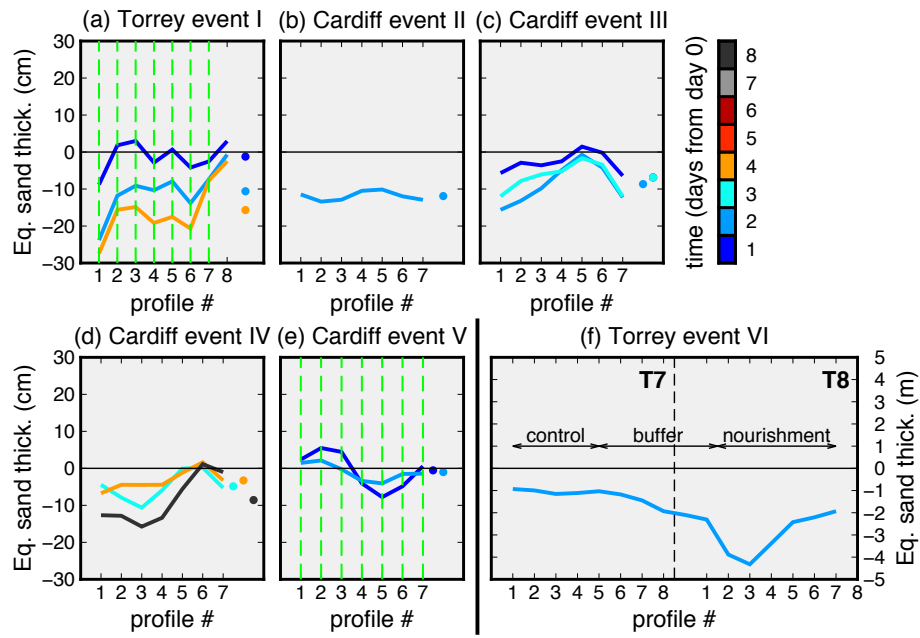10

Figure 3: Same as Fig. 2 but for C2.

Figure 4: Upper beach ($> MSL$) (equivalent) sand layer thickness change during each event, for each transect. Curve colors represent time from day 0 (see color bar). Equivalent sand thickness (ordinate) is defined as $BSC^o/(x_M - x_s^p)$, using the symbols in Equation 3. Vertical green dashed lines designate the beach profiles used to calibrate XBeach parameters (Table 2). The observed section-averaged thickness is shown as a colored circle.

12

Parameter	Values	Description
break	*roelvink1*,**roelvink2**	Wave breaking energy dissipation model
gamma	*0.42*,**0.55**	Breaker parameter in Roelvink formulation
alpha	**1**,*2*	Wave dissipation coefficient in Roelvink formulation
beta	***0.1***,0.2	Breaker slope coefficient in roller model
facAs	***0.1***,0.2,0.3,0.4	Wave asymmetry factor
hmin	0.05,***0.2***	Threshold water depth above which Stokes drift is included (m)
eps	**0.005**,*0.01*	Threshold water depth above which cells are considered wet (m)
D50	0.00016,0.00023	D50 sediment diameter (m) for Cardiff and Torrey Pines, respectively
bdslpeffmag	roelvink_bed(**roelvink_total**)	Method to apply sediment transport based on the bed slope
lws	0(**1**)	Switch to enable long wave stirring
fw	0.01(**0**)	Bed friction factor

Table 2: XBeach parameters considered in the model calibration. Boldface are the default values, italic are the optimal values based on the calibration, and values in parentheses show default values which were not considered in the model calibration.

free parameter. A single optimal set of XBeach parameters (Table 2 in italic fonts) was obtained using Torrey event I. This calibration is applied to compute all the fit measures described here for all six events tested. Further calibration details are in Appendix A.

2.6. CShore model

CShore [22, 49] is a 1-D, time-averaged sediment transport solver developed by the US Army Corps of Engineers that is recommended for FEMA assessments of foreshore and dune profile evolution [50]. Initially envisioned as a model for cross-shore nonlinear wave evolution, CShore has subsequently evolved into a modelling framework that is used to predict mean hydrodynamics, design porous coastal structures, and predict cross-shore profile development [see 22, and references therein for a detailed overview].

Here we employ the 1-D cross-shore version that estimates time-averaged quasi-stationary wave-driven hydrodynamics by forcing a mean cross-shore momentum balance with radiation stress-gradients obtained from a wave-energy balance. The average hydrodynamics are assumed in equilibrium with the average offshore forcing. Wave groups and IG waves are not modelled. Instead, IG effects on run-up and shoreline erosion are parameterized [20]. Mean hydrodynamics are used to drive a sediment transport model for a single sediment size. Specifically, cross-shore evolution is described using a bed continuity equation that relies on a parameterized description of suspended sediment fluxes in terms of hydrodynamic conditions (breaking intensity, flow strength) [51].

Cross-shore profile change is influenced most significantly by parameters governing sediment transport: a controlling efficiency of onshore transport due to velocity correlation; and e_b controlling suspension efficiency by bed stress [22]. From laboratory observations and field site calibrations (predominantly in the US East Coast) recommended values are $a \approx 0.2$, and $e_b \approx 0.005$ [22, 49]. This set of parameters, referred to as the 'Atlantic' default settings [22] which applies to beaches with pre-storm foreshore slopes of 1/18, was augmented with a set of 'Pacific' parameters that produced better fit with enhanced erosion

14

rates at Southern California beaches with milder foreshore slopes of 1/35 [22]; $a \approx 0.5$, and $e_b \approx 0.01$. These parameters enhance upper beach erosion by increasing offshore sediment fluxes. While the need for different parameter sets appears to be linked to beach slopes, the variation suggests inadequately modeled/parameterized physics.

The 1/35 foreshore slopes of the 'Pacific' sites [22, 49] are milder than the $1/20-1/30$ of the present study beaches. Simulations of the present observations using the 'Pacific' parameter set displayed nonphysically large erosion. Better agreement is found with the 'Atlantic' parameters set, in line with hypothesized foreshore slope dependence. Variation of the dominant parameters (a and e_b) around 'Atlantic' settings ($\pm80\%$ at 20% intervals) only marginally affected model skill - and improvements were uneven. We therefore evaluate CShore with default Atlantic (moderate slope) settings.

2.7. Fit measures

Model performance for profiles is quantified with the Root-Mean Square (RMS) error between the discretely sampled (at cross-shore locations $\vec{x} = [x_1, ..., x_M]$) observed ($\vec{z}^o = [z_1^o, ..., z_M^o]$) and predicted ($\vec{z}^p = [z_1^p, ..., z_M^p]$) bed elevation

$$\epsilon = \sqrt{\frac{\sum_m (z_m^p - z_m^o)^2}{m}}. \tag{1}$$

The Brier skill Score BSS is

$$skill = 1 - \frac{\epsilon^2}{\epsilon_{null}^2}, \tag{2}$$

where ϵ_{null} corresponds to RMS error of the null hypothesis, i.e. the initial profile does not change. Skill is classified as bad for $skill < 0$, poor for $skill \in [0, 0.3]$, reasonable for $skill \in (0.3, 0.6]$, good for $skill \in (0.6, 0.8]$, and excellent for $skill \in (0.8, 1]$ [52]. Skill is a popular model accuracy measure, but is sensitive to changes in a small denominator (Equation 2) [53].

Predicting shoreline erosion is of more practical importance than predicting the offshore sandbar location. Additionally, XBeach applications are often based on beach profile measurements above $\sim$ MSL [e.g. 33, 54], and many of the

15

present surveys do not extend beyond low tide (~ 2 m water depth). Model performance for shoreline volume change on multiple transects is quantified with the Bulk Shoreline Change (BSC) and Bulk Shoreline Change Error (BSCE),

$$BSC^o = \int_{x_s^p}^{x_M} (z^o - z_i)dx, \qquad BSC^p = \int_{x_s^o}^{x_M} (z^p - z_i)dx,$$
$$BSCE = \frac{\langle |BSC^p - BSC^o| \rangle}{\langle |BSC^o| \rangle}, \tag{3}$$

where superscripts o, p are observed and predicted, respectively, x_s is the shoreline position, x_M is the location of the further inland beach measurement, and z_i is the initial bed profile. $\langle \rangle$ denotes section-averaging (e.g. over all transects in a section). Note that $|BSC^p - BSC^o|$ and $|BSC^o|$ are each section-averaged before computing BSCE. BSCE results are averages over the $\sim 700 - 800$ m span of each section, and alongshore averaging reduces the sometimes erratic behavior of individual transects. BSCE is classified here as bad for $BSCE > 1$ (BSC prediction error larger than observed BSC), poor/fair for $BSCE \in [0.5, 1]$, and good/excellent for $BSCE < 0.5$.

3. Results

XBeach (calibrated and default) and CShore (Pacific and Atlantic settings) are used to predict beach profile evolution for events I to VI. Here, only calibrated XBeach and CShore with Atlantic settings are presented for events I to V. The nonphysical shoreline erosion predicted by default XBeach parameters for events I to V made it difficult to obtain a reliable skill score, which would depend on the user-defined sand availability in the upper beach (erodible sand layer thickness) and back shore. We present all model configurations for event VI (nourished profile).

3.1. Beach profile evolution

Observed section-averaged profiles for events I-V (Fig. 5(a-e)) generally exhibit a bar formation around the -2 m contour, with minor development closer

16

to the shoreline and upper beach. The offshore bar location is generally not well-predicted by XBeach, while CShore qualitatively reproduces erosion/deposition patterns well between -4 m and the shoreline for events I-V. Both XBeach and CShore generally overestimate upper beach erosion, which is moderately more pronounced for long-duration event IV. Using default parameters with XBeach and Pacific settings with CShore (not shown), the models predict large (and nonphysical) shoreline retreat for events I-V, while these settings provide better predictions for the nourished upper beach during event VI (Fig. 5(h-i)).

3.2. Skill scores

Brier skill score medians are negative for more than half of the profile test cases I to V (Fig. 6). That is, by this measure the model skill is worse than the no-change prediction. CShore produces higher median skill scores than calibrated XBeach for events I, II, III and V. XBeach arguably outperforms CShore for event IV, perhaps surprising because the event duration is longer than typical XBeach applications. CShore shows particularly high skill for Cardiff events II and V. XBeach also exhibits the highest skill for event II, and does equally well for events I, IV and V. Both models exhibit the lowest skill for event III, with XBeach BSS skills all negative, and CShore skill scores going as low as -3. For Torrey Pines event I, CShore produces poor to good skill scores for half of the beach profiles, and XBeach produces negative skill scores for all but one beach profile.

For the nourishment, Torrey event VI, BSS are given for all model configurations. Calibrated-XBeach has positive BSS in section T7, away from the nourishment, and has no skill in the nourished section T8. That is, calibrated XBeach performed well on an unnourished section in event VI, in conditions not dissimilar to calibration event I. Calibrated XBeach is here transportable, but the range of beach and wave conditions of accurate transportation is unknown. Default-XBeach on the other hand, shows high skill in the nourished section and increasingly negative skill away from the nourishment. The good performance of the (alongshore-averaged) change on the nourished section is potentially coin-
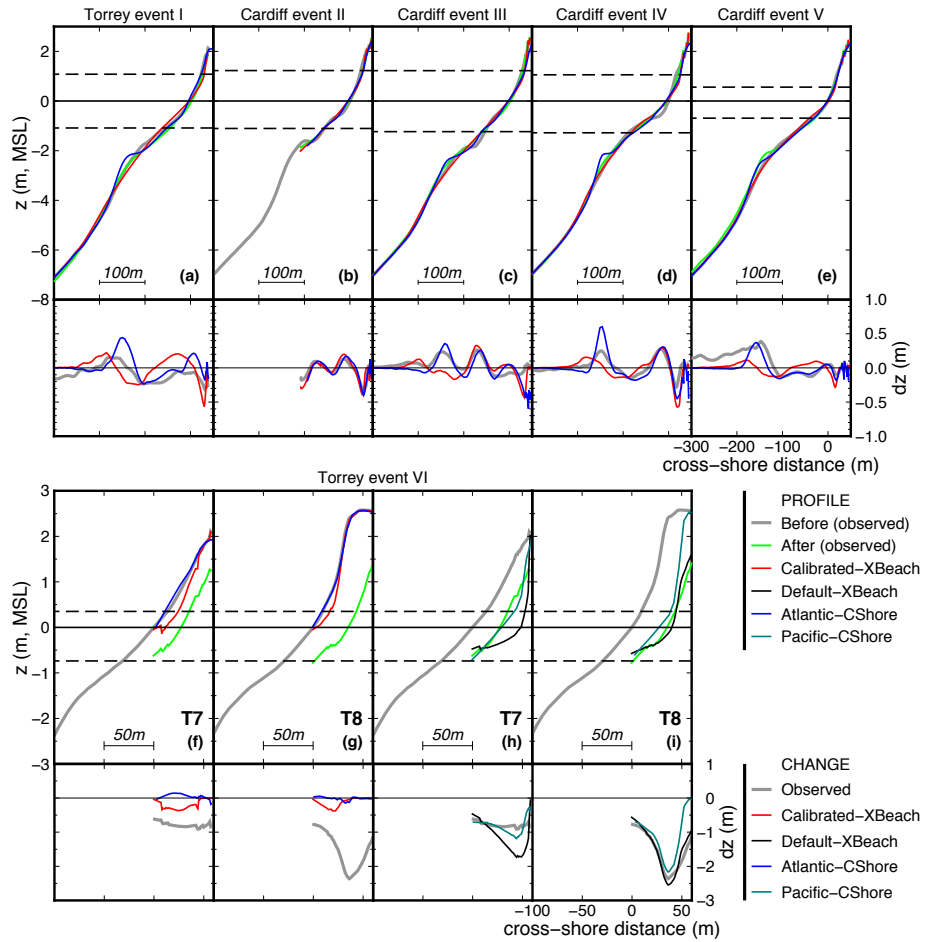
Figure 5: Section-averaged elevation (top rows) and elevation errors (bottom rows) versus cross-shore distance for all events. Top rows elevation: observed initial (gray); final observed (green), calibrated-XBeach (red), default-XBeach (black), Atlantic-CShore (blue), and Pacific-CShore (teal). Horizontal dashed lines indicate maximum and minimum observed tidal elevation during each event. Bottom rows model error: observed (gray), predicted calibrated-XBeach (red), default-XBeach (black), Atlantic-CShore (blue), and Pacific-CShore (teal) difference between initial and final bed profiles. Default-XBeach and Pacific-CShore results only shown for event VI (h&i).
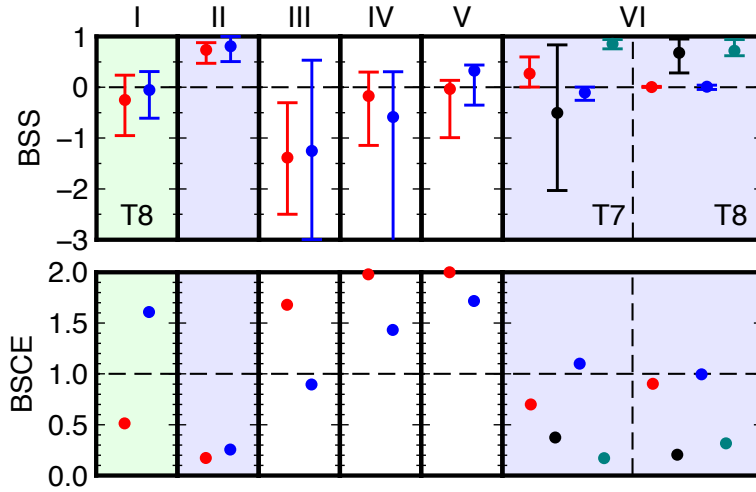
Figure 6: Section-averaged calibrated-XBeach (red), default-XBeach (black), Atlantic-CShore (blue), and Pacific-CShore (teal) fit measures for each event: skill score (BSS) of the bed elevation (Equation 2) and bulk-shoreline-change error (BSCE) of the upper beach volume (Equation 3). Bars indicate each section's minimum and maximum values. Circles in BSS plots are section median values. BSCE values exceeding 2 are displayed as 2. Green background designates the event for which XBeach parameters were calibrated and blue background designates events for which the fit measures were calculated through upper beach measurements (as opposed to full beach profiles used for all other events).

cidental. Atlantic-CShore has no skill in either T7 or T8. Pacific-CShore shows excellent skill for both sections.

The impact of parameter calibration on XBeach performance is illustrated by comparing XBeach skill scores before (e.g. default values) and after calibration (events I-V, Fig. 7) - the default-XBeach skill scores are only indicative, since the skill score computation after the upper beach is fully eroded depends on user-defined back-shore sand availability. Although calibration significantly improved skill for all profiles and events, XBeach skill remains generally low. Notably, the highest skill scores using default parameters were recorded for event V, which is of small duration and for which first-order analysis indicated a dissipative swash (section 2.4).
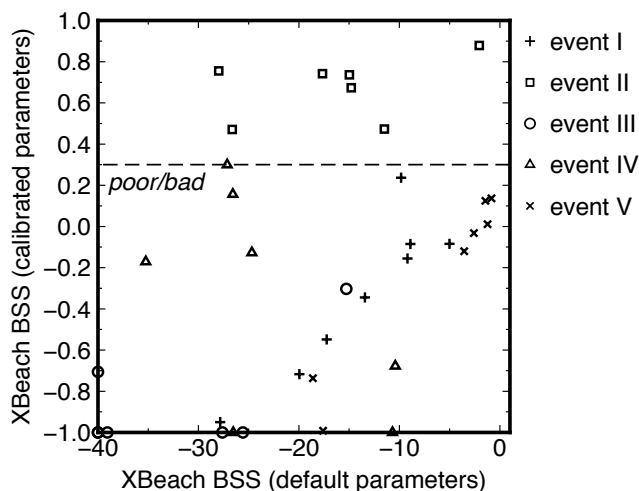
19

Figure 7: Skill of XBeach using calibrated versus default parameters. Calibrated skills less than -1 are displayed as -1. Results are shown for each transect. Only event II has skill scores > 0.3, better than bad/poor.

3.3. Predicted bulk shoreline change

The bulk-shoreline-change error (BSCE, Fig. 6 and Table 3) shows model skill in predicting erosion/accretion above MSL - the observed and predicted sand thickness change is also given (Table 4). BSCE was smaller or equal to the observed change ($BSCE \leq 1$) for three of the six events for each model. XBeach and CShore BSCE values are the largest for event V because the small observed beach volume change was predicted poorly. Both models had the lowest BSCE values for Cardiff event II, which also resulted in the highest skill. BSCE values for event I at Torrey Pines are surprisingly different between the two models, given the similar skills. CShore predicts upper beach accretion and XBeach predicts upper beach erosion (Table 4). CShore models the offshore bar evolution better, whereas XBeach models the evolution of the upper beach more accurately for event I, resulting in similar skills. The low BSCE for event VI occurs because the large observed loss of upper beach volume is predicted relatively well. Calibrated-XBeach has lower BSCE than Atlantic-CShore (Atlantic-CShore even predicts accretion for this event, Table 4), whereas default-XBeach

20

Event	I	II	III	IV	V	VI
Observed bulk shoreline change						
$\langle BSC^o \rangle$ (m^2)	-4.94	-4.98	-2.28	-2.92	-0.52	-55.42
Default-XBeach						
$\langle BSC^p \rangle$ (m^2)	-	-	-	-	-	-58.54
BSCE	-	-	-	-	-	0.25
Calibrated-XBeach						
$\langle BSC^p \rangle$ (m^2)	-6.80	-4.59	-6.12	-9.02	-3.60	-9.35
BSCE	0.51	0.17	1.68	1.98	3.70	0.85
Pacific-CShore						
$\langle BSC^p \rangle$ (m^2)	-	-	-	-	-	-44.75
BSCE	-	-	-	-	-	0.28
Atlantic-CShore						
$\langle BSC^p \rangle$ (m^2)	3.00	-4.10	-4.05	-7.34	-1.81	1.32
BSCE	1.61	0.26	0.90	1.43	1.72	1.02

Table 3: Observed and predicted section-averaged $\langle \rangle$ bulk shoreline change (BSC) and resulting bulk-shoreline-change errors (BSCE). Values for event VI provided across sections T7 and T8.

BSCE are moderately higher and lower and than Pacific-CShore in the individual sections T7 and T8, respectively (Fig. 6), and lower over both sections (Table 3).

4. Discussion

4.1. CShore performance

CShore has highly parameterized physics and low computation times; a serial run of all cases considered takes approximately an hour on a laptop computer. Arguably the model's biggest advantage is rapid computation. The drawback is that while effective when applied to well-calibrated situations, actual physics are poorly represented. Inadequate physics parameterization likely explains

21

Event	I	II	III	IV	V	VI
Observed thickness change (cm)						
Alongshore-averaged	-16	-12	-7	-9	-1	-202
Range (over transects)	(-27)-(-2)	(-13)-(-10)	(-12)-(-2)	(-16)-(1)	(-4)-(2)	(-432)-(-93)
Default-XBeach						
Alongshore-averaged	-	-	-	-	-	-223
Range (over transects)	-	-	-	-	-	(-439)-(-134)
Calibrated-XBeach						
Alongshore-averaged	-21	-11	-18	-26	-10	-39
Range (over transects)	(-25)-(-18)	(-16)-(-8)	(-25)-(-10)	(-38)-(-15)	(-13)-(-7)	(-154)-(-16)
Pacific-CShore						
Alongshore-averaged	-	-	-	-	-	-168
Range (over transects)	-	-	-	-	-	(-259)-(-116)
Atlantic-CShore						
Alongshore-averaged	9	-10	-11	-21	-5	6
Range (over transects)	(3)-(14)	(-16)-(-5)	(-14)-(-8)	(-33)-(-9)	(-7)-(-3)	(-14)-(25)

Table 4: Observed and predicted upper-beach sand thickness change during each event. Values for event VI provided across sections T7 and T8.

22

the need for two different (or more) calibration sets. However, the simplified nature of the model precludes ascertaining which critical processes are poorly represented. For example, a large proportion of swash is likely IG-driven (section 2.4), and missing IG-wave dynamics likely impart substantial error.

CShore performance can be improved by site-specific calibration. However, given the large disparity between 'Atlantic' (best for event I to V) and 'Pacific' settings (best for event VI) a unifying new set of calibration coefficients is not feasible. Variation of parameters (not shown) did not significantly improve the non-nourished cases (calibration space near optimum is flat over large range of parameters). The literature defaults are a reasonable guess of model optimum; arguably a sign of robustness of previous CShore calibration. For use in engineering practice, it is unfortunate that the application domain for Pacific and Atlantic parameters is ill-defined. Hypothesized slope dependence [22, 'Atlantic' for steep foreshore slopes, 'Pacific' for mild slopes] does not hold for our nourished case (which has a steep pre-storm foreshore). That said, the nourished beach is in an anomalous state (e.g. nourished material is less packed, grain distribution may differ, etc.), and slope dependence may hold for beaches closer to equilibrium.

4.2. XBeach performance

XBeach was principally developed for and calibrated with dissipative beach conditions, under the assumption that swash is dominated by infragravity (IG) energy [e.g. 24]. Compared with prevalent conditions along the Dutch coast (to which XBeach is typically applied), where IG-to-total significant runup R^{IG}/R is typically in the order of 0.85 [46], the considered profiles are steeper, and IG-energy is less dominant during high tide (see section 2.4). The swash zone is dissipative from start to finish only for Cardiff event V ($\xi_0 < 0.5$). In addition, XBeach application to the other events is problematic due to relatively long event duration compared to typical model applications [24, and references therein], and the relatively mild to moderate wave conditions, for which relevant physics induce beach restoration associated with nonlinear waves may be

23

missing [55]. That said, skill scores using default parameters were negative for short-duration and dissipative event V, and while the skill improved through cal-ibration, XBeach didn't perform better compared to events with less dissipative swash.

If forcing is sufficiently energetic (event VI), default XBeach performs better. Beach profile evolution was well modeled around the nourishment project (section T8 in Fig. 6) and skill scores were enhanced significantly. Bed change, however, is not only a factor of the offshore forcing and beach profile state, but also depends on erodible sand volume [56]. In this particular event, the beach was previously nourished (April 2001) in section T8, and there was sufficient upper beach sand volume to permit extensive erosion and evolve to the observed bed profile (Fig. 5(i)). Notably, on sand-depleted beach profiles, negative skills were observed for the same beach and event using default parameters (Fig. 5(h) and section T7 in Fig. 6). The default-XBeach skill scores for event VI are comparable to the XBeach results presented by Barnard et al. [31] for the common beach transects [Table 3 of 31]. However, the interpretation of the results extracted from the application of 1-D morphodynamic models for event VI should be cautious due to the unnatural beach state resulting from the nourishment project, and the strong alongshore variability of the erosion patterns observed in the field [45].

Calibration revealed that XBeach is sensitive to settings for the asymmetry scaling factor ($facAs$), and parameters controlling the energy dissipation model. More significantly, optimal parameters were also sensitive to the depth-extent of the target beach profile (Appendix A.2.1), which is largely unaddressed in literature. Studies often calibrate selected XBeach parameters based on upper beach profile measurements [e.g. 33], while limited research has considered extended [e.g. 47, 34, 27] or full beach profiles [26]. Calibrating the model parameters using upper beach (above MSL) measurements alone was shown here to yield erroneous morphological predictions below MSL for event V which resulted in little change on the upper beach (Fig. A.2(d-g)).

Best practice suggests that the parameterization of the physical processes

should be validated through field measurements before applying the model in
²⁷⁵ any new coastal site. This study revealed that site-specific calibration signif-
icantly improved the model skill. However, the disadvantage of calibration is
that model physics are no longer direct proxies for physical processes as cali-
bration tries to correct for missing physics. The net result is that calibrated-
XBeach skill did not exceed CShore skill (both are low). Future research using
³⁸⁰ XBeach2D should be undertaken to include the effect of directional spreading
on groupiness of the short waves [24], and the long-shore effects introduced by
along-shore variations in the nearshore bathymetry/topography [56].

5. Conclusions

Two widely used process-based numerical models, XBeach and CShore, were
³⁸⁵ used to simulate morphological evolution of two southern California beaches.
The model predictions were compared to beach profile observations for six wave
events of varying duration and characteristics of typical winter storms; long
period swell ($T_p \sim$ 9-17 s) with moderate peak H_s($\sim$ 1.7-3 m), and moderate
foreshore beach slope (1/20-1/30). Default XBeach performance was poor for
³⁹⁰ five of the six events, likely because the events considered were suboptimal for
XBeach applications (ideally waves with large H_s and short wave periods on
relatively-low foreshore slopes, for short durations).

XBeach model parameters were therefore calibrated for these moderately
energetic storm events. Optimized parameters improved model predictions, but
³⁹⁵ skill was still often low. CShore default settings yielded comparable skill scores
to calibrated-XBeach, while selection between the two alternative parameter sets
('Pacific' or 'Atlantic') was non-obvious. Using optimum parameters, CShore
predicted the evolution of the full beach profile more accurately than calibrated
XBeach for three of the five moderate events, but skill was low. The evolution
⁴⁰⁰ of the observed offshore bar is captured well by CShore. The upper beach
volume change error of both CShore and XBeach was smaller or equal to the
observed change for only two out of the five moderate storm events tested.

25

The alongshore variability of upper beach and offshore bar response was not adequately resolved with either XBeach or CShore 1-D simulations using a single set of model parameters. In their present forms, CShore and XBeach preclude detailed physics-based sediment transport and beach profile investigations on these typical southern California beaches, but may provide useful qualitative estimates.

The large volume of XBeach applications (in the academic literature and practice) highlights the community need for open source, physics-based models to predict the morphological evolution of sandy beaches during storms. Reducing the complexity of the physical processes involved, ultimately restricts the validity of the model, or at least the validity of default settings of the free parameters. While this study demonstrates that the morphological predictions of XBeach and CShore are comparable for moderate storm events on mildly-dissipative to dissipative beaches, the models were not tested for the mild-sloping foreshores and typical energetic sea-dominated storms for which XBeach was developed. Clarity on the restrictions of application is important for both models' successful implementation and to bring applications into a unified context.

6. Acknowledgements

Cardiff. Kathleen Ritzman, Scripps Assistant Director, was essential to maintaining funding and survey continuity.

References

[1] Pendleton L, Kildow J. The non-market value of beach recreation in california. Shore and Beach 2006;74(2):34–7.

[2] Church J, Clark P, Cazenave A, Gregory J, Jevrejeva S, Levermann A, et al. Sea level change. In: Stocker T F, Qin D, Plattner G K, Tignor M, Allen S, Boschung J, Nauels A, Xia Y, Bex V, Midgley P (eds) Climate change 2013: the physical science basis. Contribution of Working Group I to the Fifth Assessment Report of the Intergovernmental Panel on Climate Change. Cambridge University Press, Cambridge and New York; 2013, p. 1137–216.

[3] Hansen J, Sato M, Hearty P, Ruedy R, Kelley M, Masson-Delmotte V, et al. Ice melt, sea level rise and superstorms: evidence from paleoclimate data, climate modeling, and modern observations that 2 °c global warming could be dangerous. Atmospheric Chemistry and Physics 2016;16(6):3761–812. doi:`10.5194/acp-16-3761-2016`.

[4] DeConto RM, Pollard D. Contribution of antarctica to past and future sea-level rise. Nature 2016;531(3):591 –7. doi:`10.1038/nature17145`.

[5] Carson M, Köhl A, Stammer D, Slangen ABA, Katsman CA, van de Wal RSW, et al. Coastal sea level changes, observed and projected during the 20th and 21st century. Climatic Change 2016;134(1):269–81. doi:`10.1007/s10584-015-1520-1`.

[6] Tebaldi C, Strauss BH, Zervas CE. Modelling sea level rise impacts on storm surges along us coasts. Environmental Research Letters 2012;7(1):014032.

[7] Cai W, Borlace S, Lengaigne M, van Rensch P, Collins M, Vecchi G, et al. Increasing frequency of extreme el niño events due to greenhouse warming. Nature Climate Change 2014;4:111–6. doi:10.1038/nclimate2100.

[8] Seymour RJ, Strange RR, Cayan DR, Nathan RA. Influence of El Niños on California's wave climate. In Billy L. Edge, ed. 1984. Nineteenth Coastal Engineering Conference: Proceedings of the International Conference. New York: ASCE: 557-592; 1984,.

[9] Ludka BC, Gallien TW, Crosby SC, Guza RT. Mid-el niño erosion at nourished and unnourished southern california beaches. Geophysical Research Letters 2016;43(9):4510–6. doi:10.1002/2016GL068612.

[10] Barnard PL, Hoover D, Hubbard DM, Snyder A, Ludka BC, Allan J, et al. Extreme oceanographic forcing and coastal response due to the 2015-2016 el niño. Nature Communications 2017;8(14365). doi:10.1038/ncomms14365.

[11] Nicholls RJ, Cazenave A. Sea-level rise and its impact on coastal zones. Science 2010;328(5985):1517–20. doi:10.1126/science.1185782.

[12] Wright LD, Short AD. Morphodynamic variability of surf zones and beaches: A synthesis. Marine Geology 1984;56(1):93–118. doi:10.1016/0025-3227(84)90008-2.

[13] Larson P, Kraus NC. SBEACH: Numerical model for simulating storm-induced beach change; Report 1, Empirical foundation and model development. Technical Report CERC-89-9. U.S. Army Engineer Waterways Experiment Station, Coastal Engineering Research Center, Vicksburg, MS.; 1989,.

[14] Plant NG, Holman RA, Freilich MH, Birkemeier WA. A simple model for interannual sandbar behavior. Journal of Geophysical Research: Oceans 1999;104(C7):15755–76. doi:10.1029/1999JC900112.

28

[15] Ludka BC, Guza RT, O'Reilly WC, Yates ML. Field evidence of beach profile evolution toward equilibrium. Journal of Geophysical Research Oceans 2015;120:7574–97. doi:10.1002/2015JC010893.

[16] Dong P, Zhang K. Intense near-bed sediment motions in waves and currents. Coastal Engineering 2002;45(2):75 – 87. doi:10.1016/S0378-3839(02)00040-6.

[17] Hsu TJ, Jenkins JT, Liu PLF. On two-phase sediment transport: sheet flow of massive particles. Proceedings of the Royal Society of London A: Mathematical, Physical and Engineering Sciences 2004;460(2048):2223–50. doi:10.1098/rspa.2003.1273.

[18] Gonzalez-Ondina JM, Fraccarollo L, Liu PLF. Two-level, two-phase model for intense, turbulent sediment transport. Journal of Fluid Mechanics 2018;839:198238. doi:10.1017/jfm.2017.920.

[19] Kim Y, Cheng Z, Hsu TJ, Chauchat J. A numerical study of sheet flow under monochromatic nonbreaking waves using a free surface resolving eulerian two-phase flow model. Journal of Geophysical Research: Oceans 2018;123(7):4693–719. doi:10.1029/2018JC013930.

[20] Kobayashi N. Efficient wave and current models for coastal structures and sediments, Nonlinear Wave Dynamics. World Scientific; 2008, p. 67–87. doi:10.1142/9789812709042_0003.

[21] Roelvink D, Reniers A, van Dongeren A, van Thiel de Vries J, McCall R, Lescinski J. Modelling storm impacts on beaches, dunes and barrier islands. Coastal Engineering 2009;56(11):1133 –52. doi:10.1016/j.coastaleng.2009.08.006.

[22] Johnson BD, Kobayashi N, Gravens MB. Cross-shore numerical model CSHORE for waves, currents, sediment transport and beach profile evolution, Final Rep. No. ERDC/CHL TR-12-22. U.S. Army Corps of Engineers, Coastal and Hydraulics Laboratory, Vicksburg, MS; 2012,.

29

[23] Roelvink D, van Dongeren A, McCall R, Hoonhout B, van Rooijen A, van Geer P, et al. XBeach Technical Reference: Kingsday Release. Model description and functionalities. Deltares, Delft, ND.; 2015,.

[24] Roelvink D, McCall R, Mehvar S, Nederhoff K, Dastgheib A. Improving predictions of swash dynamics in xbeach: The role of groupiness and incident-band runup. Coastal Engineering 2018;134:103 –23. doi:10.1016/j.coastaleng.2017.07.004.

[25] de Winter R, Gongriep F, Ruessink B. Observations and modeling of alongshore variability in dune erosion at egmond aan zee, the netherlands. Coastal Engineering 2015;99:167 –75. doi:10.1016/j.coastaleng.2015.02.005.

[26] Vousdoukas MI, Ferreira O, Almeida LP, Pacheco A. Toward reliable storm-hazard forecasts: Xbeach calibration and its potential application in an operational early-warning system. Ocean Dynamics 2012;62:1001–15. doi:10.1007/s10236-012-0544-6.

[27] Armaroli C, Grottoli E, Harley MD, Ciavola P. Beach morphodynamics and types of foredune erosion generated by storms along the emilia-romagna coastline, italy. Geomorphology 2013;199:22 – 35. doi:10.1016/j.geomorph.2013.04.034.

[28] Harter C, Figlus J. Numerical modeling of the morphodynamic response of a low-lying barrier island beach and foredune system inundated during hurricane ike using xbeach and cshore. Coastal Engineering 2017;120:64 – 74. doi:10.1016/j.coastaleng.2016.11.005.

[29] Yates ML, Guza RT, O'Reilly WC, Seymour RJ. Overview of seasonal sand level changes on southern california beaches. Shore and Beach 2009;77(1):39–46.

[30] Wright L, Short A, Green M. Short-term changes in the morphodynamic

states of beaches and surf zones: An empirical predictive model. Marine Geology 1985;62(3):339 –64. doi:10.1016/0025-3227(85)90123-9.

[31] Barnard PL, van Ormondt M, Erikson LH, Eshleman J, Hapke C, Ruggiero P, et al. Development of the coastal storm modeling system (cosmos) for predicting the impact of storms on high-energy, active-margin coasts. Natural Hazards 2014;74(2):1095–125. doi:10.1007/s11069-014-1236-y.

[32] O'Neill AC, Erikson LH, Barnard PL, Limber PW, Vitousek S, Warrick JA, et al. Projected 21st century coastal flooding in the southern california bight. part 1: Development of the third generation cosmos model. Journal of Marine Science and Engineering 2018;6(2). doi:10.3390/jmse6020059.

[33] Splinter KD, Palmsten ML. Modeling dune response to an east coast low. Marine Geology 2012;329-331:46–57. doi:10.1016/j.margeo.2012.09.005.

[34] Callaghan DP, Ranasinghe R, Roelvink D. Probabilistic estimation of storm erosion using analytical, semi-empirical, and process based storm erosion models. Coastal Engineering 2013;82:64–75. doi:10.1016/j.coastaleng.2013.08.007.

[35] Smallegan SM, Irish JL, Dongeren AV, Bieman JPD. Morphological response of a sandy barrier island with a buried seawall during hurricane sandy. Coastal Engineering 2016;110:102 –10. doi:10.1016/j.coastaleng.2016.01.005.

[36] Raubenheimer B, Guza RT. Observations and predictions of runup. Journal of Geophysical Research: Oceans 1996;101(C11):25575–87. doi:10.1029/96JC02432.

[37] Moffatt and Nichol . Coastal regional sediment management plan for the San Diego region. Tech. Rep. 6731-01, SANDAG, Long Beach, Calif.; 2010,.

[38] Ludka BC, Guza RT, O'Reilly WC. Nourishment evolution and impacts at four southern california beaches: A sand volume analysis. Coastal Engineering 2018;136:96 – 105. doi:`10.1016/j.coastaleng.2018.02.003`.

[39] Adams PN, Inman DL, Graham NE. Southern california deep-water wave climate: Characterization and application to coastal processes. Journal of Coastal Research 2008;24:1022–35. doi:`10.2112/07-0831.1`.

[40] O'Reilly WC, Guza RT. Assimilating coastal-wave observations in regional swell predictions. part i: Inverse methods. Journal of Physical Oceanography 1998;28:679–91. doi:`10.1175/1520-0485(1998)028<0679: ACWOIR>2.0.CO;2`.

[41] O'Reilly WC, Olfe CB, Thomas J, J.Seymour R, Guza RT. The california coastal wave monitoring and prediction system. Coastal Engineering 2016;116:118–32. doi:`10.1016/j.coastaleng.2016.06.005`.

[42] Lygre A, Krogstad HE. Maximum entropy estimation of the directional distribution in ocean wave spectra. Journal of Physical Oceanography 1986;16:2052–60. doi:`10.1175/1520-0485(1986)016<2052:MEEOTD>2.0. CO;2`.

[43] Yates ML, Guza RT, Seymour R. Seasonal persistence of a small southern california beach fill. Coastal Engineering 2009;56:559 –64. doi:`10.1016/j. coastaleng.2008.11.004`.

[44] Yates ML, Guza RT, O'Reilly WC, Hansen JE, Barnard PL. Equilibrium shoreline response of a high wave energy beach. Journal of Geophysical Research: Oceans 2011;116(C4). doi:`10.1029/2010JC006681`.

[45] Seymour R, Guza RT, O'Reilly W, Elgar S. Rapid erosion of a small southern california beach fill. Coastal Engineering 2005;52:151 –8. doi:`10. 1016/j.coastaleng.2004.10.003`.

32

[46] Ruessink BG, Kleinhans MG, van den Beukel PGL. Observations of swash under highly dissipative conditions. Journal of Geophysical Research: Oceans 1998;103(C2):3111–8. doi:`10.1029/97JC02791`.

[47] McCall RT, van Thiel de Vries JSM, Plant NG, van Dongeren AR, Roelvink JA, Thompson DM, et al. Two-dimensional time dependent hurricane overwash and erosion modeling at santa rosa island. Coastal Engineering 2010;57:668–83. doi:`10.1016/j.coastaleng.2010.02.006`.

[48] Roelvink D, Reniers A, van Dongeren A, van Thiel de Vries J, Lescinski J, McCall R. XBeach Model Description and Manual - V6. Deltares, Delft, ND.; 2010,.

[49] Kobayashi N. Coastal sediment transport modeling for engineering applications. Journal of Waterway, Port, Coastal, and Ocean Engineering 2016;142(6):03116001. doi:`10.1061/(ASCE)WW.1943-5460.0000347`.

[50] FEMA . Guidance for Flood Risk Analysis and Mapping: Coastal Erosion. Risk Mapping, Assessment and Planning (Risk MAO) Program. Federal Emergency Management Agency (FEMA); 2018,.

[51] Kobayashi N, Johnson BD. Sand suspension, storage, advection, and settling in surf and swash zones. Journal of Geophysical Research: Oceans 2001;106(C5):9363–76. doi:`10.1029/2000JC000557`.

[52] van Rijn LC, Walstra DJR, Grasmeijer B, Sutherland J, Pan S, Sierra JP. The predictability of cross-shore bed evolution of sandy beaches at the time scale of storms and seasons using process-based profile models. Coastal Engineering 2003;47:295–327. doi:`10.1016/S0378-3839(02)00120-5`.

[53] Sutherland J, Peet AH, Soulsby RL. Evaluating the performance of morphological models. Coastal Engineering 2004;51(8):917 –39. doi:`10.1016/j.coastaleng.2004.07.015`.

[54] Dissanayake P, Brown J, Karunarathna H. Impacts of storm chronology on the morphological changes of the formby beach and dune sys-

tem, uk. Nat Hazartds Earth Syst Sci 2015;15:1553–43. doi:`10.5194/`
`nhess-15-1533-2015`.

[55] van Thiel de Vries JSM. Dune erosion during storm surges. Ph.D. thesis; Delf University of Technology; 2009.

[56] van Thiel de Vries JSM, van Dongeren AR, McCall RT, Reniers AJHM. The effect of the longshore dimension on dune erosion. Coastal Engineering Proceedings 2011;32:sediment.49. doi:`10.9753/icce.v32.sediment.49`.

[57] Roelvink JA. Dissipation in random wave groups incident on a beach. Coastal Engineering 1993;19:127–50. doi:`10.1016/0378-3839(93)90021-Y`.

[58] Thornton EB, Guza RT. Energy saturation and phase speeds measured on a natural beach. Journal of Geophysical Research 1982;87:9499–508. doi:`10.1029/JC087iC12p09499`.

[59] Stockdon HF, Thompson DM, Plant NG, Long JW. Observations of wave runup, setup, and swash on natural beaches. Coastal Engineering 2014;92:1 – 11. doi:`10.1016/j.coastaleng.2014.06.004`.

[60] Raubenheimer B, Guza RT, Elgar S. Field observations of wavedriven setdown and setup. Journal of Geophysical Research: Oceans 2001;106(C3):4629–38. doi:`10.1029/2000JC000572`.

[61] Thornton EB, Guza RT. Transformation of wave height distribution. Journal of Geophysical Research 1983;88:5925–38. doi:`10.1029/JC088iC10p05925`.

[62] Pender D, Karunarathna H. A statistical-process based approach for modelling beach profile variability. Coastal Engineering 2013;81:19 – 29. doi:`10.1016/j.coastaleng.2013.06.006`.

[63] Harley M, Armaroli C, Ciavola P. Evaluation of xbeach predictions for a real-time warning system in emilia-romagna, northern italy. Journal of Coastal Research 2011;SI 64:1861 –5.

34

Appendix A. XBeach calibration

Appendix A.1. Calibration parameters

Calibrated XBeach parameters are described briefly. Roelvink et al. [23]
provides details. See Table 2 for the parameter values tested.

break	Toggle between the Roelvink [57] wave breaking energy dissipation model (*break = roelvink*1) and a formulation proportional to H^3/h instead of H^2 (*break = roelvink*2), where H is the wave height and h is the local water depth.
gamma	Wave breaking parameter. Higher *gamma* yields less energy dissipation from wave breaking. Default *gamma* = 0.55 [57] uses field and laboratory data, whereas *gamma* = 0.42 is based on the Torrey Pines beach observations [58]. Stockdon et al. [59] showed XBeach swash predictions of the SandyDuck field observations [60] were best using *gamma* = 0.42.
alpha	O(1) wave dissipation coefficient in the wave breaking formulations described above.
beta	Breaker slope coefficient in the roller energy dissipation equation. Increasing *beta* shifts the setup forcing offshore.
fw	Bed friction factor in the wave action equation. Default is $fw = 0$. We use $fw = 0.01$, an accepted nominal value, although frictional dissipation is expected to be much smaller than the dissipation due to wave breaking [61].
lws	Toggle for long wave stirring affects the formulation of the velocity magnitude, which in turn is used to compute the equilibrium sediment concentration. $lws = 0$ was used based on preliminary simulations which consistently showed that this option produced higher skill scores during calm and moderate conditions.

bdslpeffmag	Toggle to apply bed slope effect magnitude correction to the total sediment transport (default), or only on the bed load transport ($bdslpeffmag = roelvink\_bed$). The latter was chosen for the relatively steep swash zones of this study (as recommended by R. McCall, personal communication).
facAs	Wave asymmetry scaling factor. Higher $facAs$ values lead to higher onshore sediment transport by short waves asymmetry). Default $facAs = 0.1$, but larger values have been used for steeper (non-dissipative) beaches [e.g. 26], or to simulate beach recovery [e.g. 62].
hmin	Threshold water depth to include Stokes drift limits unrealistically-high return flow velocities in very shallow water. Range considered $hmin = 0.05 - 0.2$, [e.g. 34].
eps	Threshold water depth for wetting and drying. Range considered $eps = 0.005 - 0.01$, [e.g. 63].
D50	Uniform D50 sediment diameter. It is set at 0.16 and 0.23 mm for Cardiff and Torrey Pines, respectively [15].

Appendix A.2. Calibration Results

XBeach was developed to simulate dune erosion, overwash and breaching during extreme events [48]. Most XBeach parameter calibrations are based on beach profile measurements above $\sim$ MSL [e.g. 33, 54]. Similar to the literature, calibration here is developed on the upper beach, but a calibration that spans the beach is also performed where extended and full beach profiles are available. Ultimately, the optimal set of XBeach parameters based on the full beach profile calibration at day 4 of Torrey event I is applied to all other events, and to shoreline erosion (BSCE).

To consider sensitivity of calibration optimum to the profile extent used to evaluate skill, XBeach was calibrated with: 1) upper beach bed elevations ($z \geq$MSL); 2) swash-zone bed elevations (defined as tidal elevation and setup plus or minus half a significant wave height, or the extent of bed elevation

36

measurements, whichever is smaller); and 3) full beach profiles. All seven Cardiff profiles of section C2 and seven selected beach profiles from section T8 at Torrey Pines (Fig. 4) were used for the calibration. Skill calculation is expanded across multiple ($N = 7$) profiles to produce a skill score for each evaluation day (i):

$$\text{skill}^i = 1 - \frac{\sum_{n=1}^{7}(\epsilon_n^i)^2}{\sum_{n=1}^{7}(\epsilon_{n,\text{null}}^i)^2}. \tag{A.1}$$

660   Skill scores were calculated for all combinations of the parameters given in Table 2, and maximum skill scores were used to determine the optimal XBeach parameters. To illustrate sensitivity to different parameter choices, maximum skill scores for each fixed parameter are shown where the model predictions resulting from all combinations of parameters that include this particular pa-

665   rameter value. Maximum skill scores for each parameter are calculated from model predictions with that parameter held constant, and the other free parameters varied over all combinations. Searching over all possible parameter combinations yields the optimal combination of parameters (Table 2).

XBeach Skill score distributions are significantly affected by *facAs*, *gamma*,

670   *break* and *alpha* (Fig. A.1). Further, at Cardiff sensitivity to *hmin* and *eps* is more significant due to the smaller change in upper beach volume. The upper beach for Torrey Pines event I is more sensitive to *alpha* and *beta*. In terms of the optimal parameter combinations (max BSS), *facAs*, *gamma* and *break* dominate. The max BSS favor higher *facAs* for the upper beach and swash-

675   zone calibrations of event V at Cardiff compared to event I at Torrey Pines, which can be attributed to the greater upper beach erosion measured at Torrey Pines (Fig. 4(a&e)).

Max BSS distributions remain relatively constant throughout the duration of the two calibration events, even though the offshore forcing varies significantly.

680   Based on the evidence of the more frequently-assessed upper beach skill, max BSS does not appear to decrease with time due to the cumulative bed-profile prediction error for either of the two events. Optimal parameters resulting from the full profile calibrations at day 4 of event I and day 2 of event V are identical, with the exception of parameter *alpha*. The set of Torrey Pines optimal
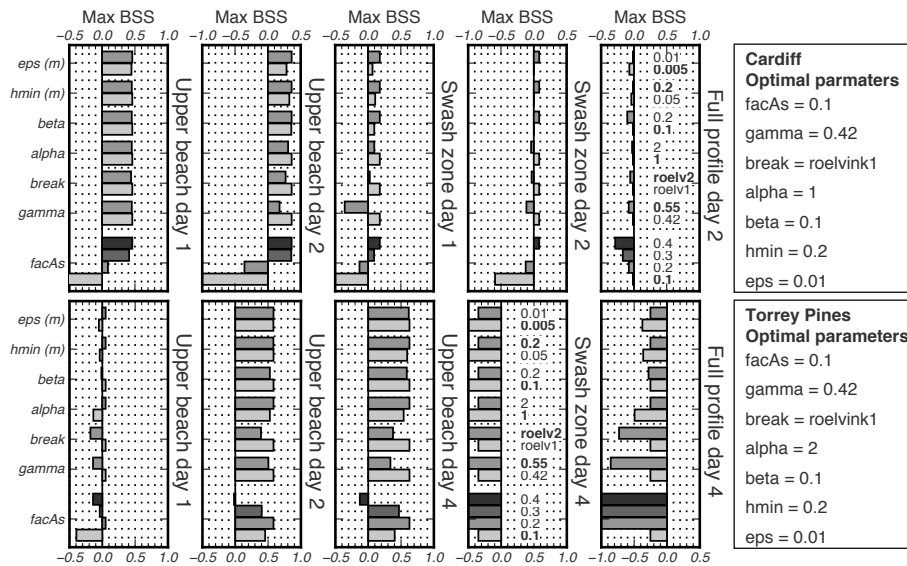
37

Figure A.1: XBeach calibration results for the Cardiff event V and Torrey Pines event I : 7-profile-total XBeach skill scores for all 256 combinations of the XBeach parameters (Table 2). The default parameter values are in boldface.

parameters was selected because of the higher relative preference for *alpha*= 2. The calibration results show that *gamma* = 0.42 results in more accurate morphodynamic predictions for beaches in southern California, at least for the moderate storm events tested here, which agrees with the field observations of Thornton and Guza [58] in the study area.

Appendix A.2.1. Sensitivity to profile extent

Sensitivity of calibration optimum parameters (and skill) to profile extent used in skill score calculations is investigated by considering calibration profiles defined by the upper beach, the swash-zone and full observed profiles. Focusing on the optimal parameters (max BSS) of day 2 at Cardiff (Fig. A.1), the upper beach and swash zone calibrations yield different parameter optima than full profile calibration. Since the upper beach sand volume doesn't change significantly at Cardiff during the two-day event (Fig. 4(e)), more onshore sediment transport (higher *facAs*) is required to stabilize the upper beach profile. The

38

optimal $facAs = 0.1$ and $gamma = 0.42$ resulting from the full profile pa-
rameter calibration predict erosion on the upper beach at day 2, but produce
a more balanced beach profile at depths below MSL (Fig. A.2), although off-
shore sandbar formation is not captured well by the model (Fig. 5(e)). On
the other hand, increasing the wave asymmetry factor to the upper beach cali-
bration optimal value ($facAs = 0.4$) may unrealistically distort the bed profile
below MSL (e.g. Fig. A.2(d-g)). While for this event the optimal parameters
for the swash zone are identical to the optimal parameters resulting from the
upper beach calibration, depending on the offshore depth limit of the swash
zone, the optimal parameters based on the swash zone calibration may sway
towards the upper beach or full profile optimal parameters. At Torrey Pines,
the upper beach parameter calibration yields different optimal values than the
swash zone calibration for the *facAs*, *beta* and *eps* parameters.

Appendix A.2.2. Alongshore variability and sensitivity to 2-D effects

The beach response to the storm events varies alongshore (Fig. 4). At Tor-
rey Pines, where the alongshore variation is more pronounced, the upper beach
generally erodes, but not equally at each transect (Fig. 4(a) and Table 4). Dur-
ing event V at Cardiff, some of the beach profiles along section C2 experienced
upper beach accretion and others erosion (Fig. 4(e) and Table 4). Contributing
factors to the beach response alongshore variation include alongshore variations
in bathymetry and upper beach topography, which induce long-shore sediment
transport [56]. Since 2-D neasrshore effects are not captured in the 1-D XBeach
simulations presented here, the optimal model parameters based on the mea-
sured beach profiles vary alongshore to compensate for the missing forcing input
(Fig. A.3). Optimizing the XBeach parameters on individual beach profiles gen-
erally resulted in higher skill scores than the skill score computed across multiple
beach profiles through Equation A.1 (Fig. A.3). For the wave conditions tested
here, XBeach presents a low (total) skill in predicting the bed evolution across
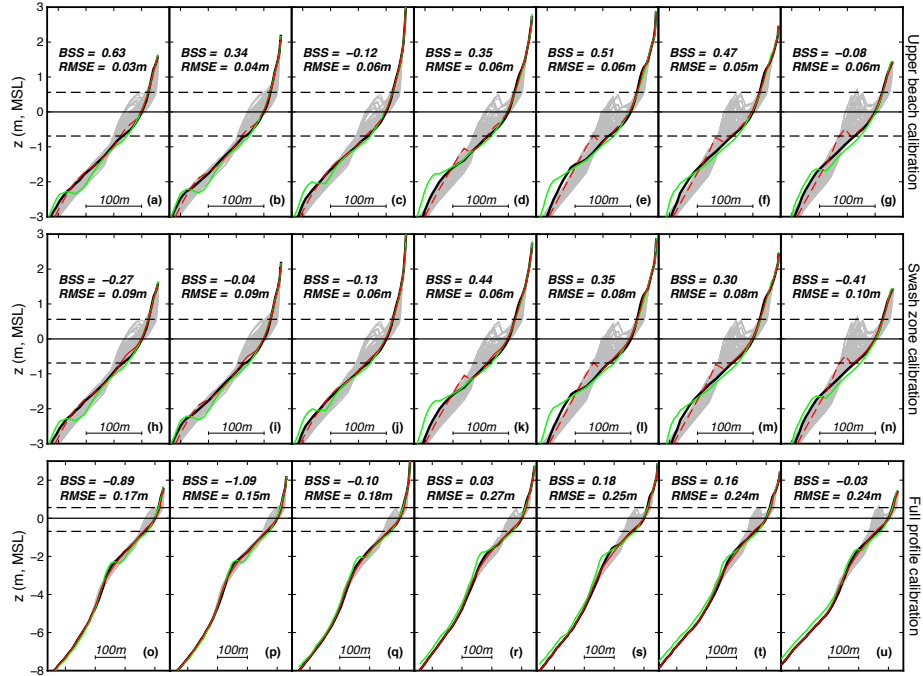multiple beach profiles for a single set of parameters in the presence of 2-D
effects.

39

Figure A.2: Beach profiles for the XBeach parameter calibration corresponding to day 2 of the Cardiff event V; sub-plots (a) and (g) correspond to the southern-most (C2-1) and northern-most (C2-7) beach profiles, respectively. Black line: measured beach profile at day 0; Green line: measured beach profile at day 2; Gray lines: XBeach bed elevation predictions for all combination of parameters given in Table 2; Red line: optimal XBeach-predicted beach profile for each depth-extent based on the 7 profile-averaged skill scores (the continuous red line corresponds to the beach profile segment used to calculate the skill score, and the red dashed line is its extension along the full beach profile). Black horizontal dashed lines correspond to the minimum and maximum tidal elevations during the simulation.
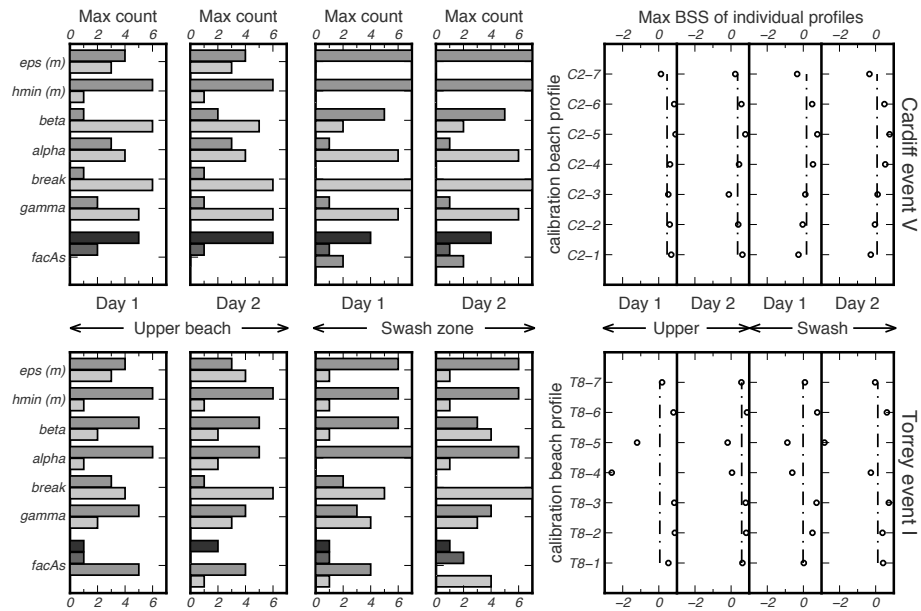
Figure A.3: Alongshore variability of optimal XBeach parameters computed from the seven beach profiles used for the calibration at Cardiff (top row) and Torrey Pines (bottom row). The left group of plot shows the number of profiles (out of seven) for which each parameter value provided the maximum skill score (max count). The right plots show a comparison between the maximum skill score at each individual beach profile (circles) and the total skill score (dash-dot line) computed using Equation A.1. Separate skill scores are shown in each sub-plot for each of the two event days, for the upper beach and swash zone.